On the mixing of a confined stratified fluid by a turbulent buoyant plume

RICHARD W. MOTT† AND ANDREW W. WOODS

BP Institute, Madingley Rise, Cambridge CB3 0EZ, UK

We investigate the mixing of a stratified fluid of finite volume by a turbulent buoyant plume. We develop a model to describe the mixing and apply this to both the cases of a two-layer stratification and a continuous stratification. With a two-layer stratification, the plume intrudes at the interface where it supplies an intermediate layer of fluid. This new layer gradually deepens, primarily mixing the original near-source layer of fluid through entrainment. Eventually, this intermediate layer becomes sufficiently buoyant that the plume penetrates into the more distal layer, leaving a partially mixed region between the original layers of fluid. Analysis of new experiments shows that the growth of the intermediate layer depends primarily on the ratio λ of (i) the filling box time, during which the plume entrains a volume of fluid equal to that in the near-source layer, and (ii) the time for the buoyancy of the near-source layer to increase to that of the more distal layer. For small values of λ, the near-source layer becomes approximately well mixed, and the penetration time of the plume scales with the buoyancy evolution time of the near-source layer. In the limit $\lambda \sim O(1)$, however, the plume penetrates through into the distal layer long before the near-source layer becomes well mixed; instead, at the time of penetration, the plume leaves an intermediate partially mixed zone between the two original layers. We develop a new phenomenological model to account for the mixing in this intermediate layer based on the effective turbulent diffusion associated with the kinetic energy in the plume and compare this with the model for penetrative entrainment proposed by Kumagai (*J. Fluid Mech.*, vol. 147, 1984, p. 105). In comparison with the experimental data, the models provide a reasonably accurate prediction of the plume penetration time, while the diffusive mixing model provides a somewhat more accurate description of the evolution of the density profile for a range $0 < \lambda < 1$. The diffusive mixing model also leads to predictions which are consistent with some new experimental data for the case in which a plume mixes a continuously stratified layer. In particular, the model is able to predict the initial transient mixing of the region between the source and the height at which the plume intrudes laterally in the ambient fluid, thereby providing an advance on the late-time mixing model of Cardoso and Woods (*J. Fluid Mech.*, vol. 250, 1993, p. 277). We consider the implications of these results on the turbulent penetrative entrainment associated with buoyant plumes.

1. Introduction

In many geophysical and environmental situations, local sources of buoyancy generate turbulent buoyant plumes which entrain large volumes of fluid (Turner 1979).

† Email address for correspondence: richard.mott@bpi.cam.ac.uk

In a confined enclosure, with an ambient fluid of uniform density, such plumes entrain a volume of fluid comparable to the volume of the container over a time scale known as the filling box time (Baines & Turner 1969). As a result, over this time scale, the buoyancy becomes mixed throughout the ambient fluid. Important examples of such mixing include the downward mixing of cold air from an air-conditioning system in a large auditorium (Linden 1999; Fitzgerald & Woods 2007), the downward mixing of dense plumes in the polar oceans (Paluskiiewicz, Garwood & Denbo 1994), the eruption of CO_2 saturated lakes (Woods & Phillips 1999) and the mixing which arises when hot buoyant magma is injected into an existing hot magma chamber (Phillips & Woods 2001). Also, in some situations, chemical reactions may arise from the mixing produced by turbulent plumes (Conroy, Llewellyn-Smith & Caulfield 2005).

In many of these cases, however, the ambient fluid may be initially stratified in density. This acts to arrest the motion of the plume and a laterally spreading intrusion develops at the so-called neutral buoyancy height in the ambient fluid (Morton, Taylor & Turner 1956), thereby changing the subsequent mixing process depending on the nature of the stratification. To explore this in more detail, it is useful to consider two end-member situations, a two-layer stratification and a continuous stratification. In the remainder of our discussion, we consider a relatively dense plume descending through a stably stratified ambient fluid, although the discussion is equally applicable to ascending plumes of relatively buoyant fluid.

With a two-layer stratification, if the plume is initially buoyant when it first reaches the interface with the lower layer ($\lambda < 1$), then it intrudes at the interface with the original lower layer. A new intermediate layer then gradually deepens as it incorporates progressively more of the fluid between the source and the interface through entrainment by the plume (figure 1a). Since the intermediate layer contains all the buoyant fluid supplied from the source, the mean buoyancy of the plume decreases more slowly with depth once it has entered this intermediate layer. As a result, there is a critical time at which the mean buoyancy of the plume in fact remains greater than that of the original lower layer when it reaches the interface between the intermediate and lower layers.

Subsequently, we expect the plume to penetrate through the interface and descend through the lower layer. We note that in practice just prior to the transition, some of the plume fluid may be denser than the density of the lower layer owing to the turbulent fluctuations within the plume. As a result, there may be a small amount of mixing into the lower layer, but the majority of the plume fluid intrudes at the interface until the main penetration event.

Kumagai (1984) studied this mixing process in the limit such that the buoyancy contrast between the upper and lower layers was much larger than the initial buoyancy of the plume at interface, relative to the upper layer. As a result, the plume continued to intrude at the interface between the layers, leading to mixing of the upper layer through the filling box process (cf. Baines & Turner 1969) with a gradual increase in its buoyancy. Plume breakthrough then only occurred once the upper layer buoyancy became similar to that of the lower layer. In the more general case that the initial density of the plume at the interface between the two layers is similar to (but less than) that of the lower layer, plume breakthrough may occur long before the upper layer buoyancy has evolved to that of the lower layer. In this case, the intermediate layer may only grow by a relatively small amount before the plume breakthrough. The main content of this paper is concerned with exploring this mixing process.

First, we identify a dimensionless parameter which has a strong control on the evolution of the intermediate mixed layer. We then present a systematic series of new
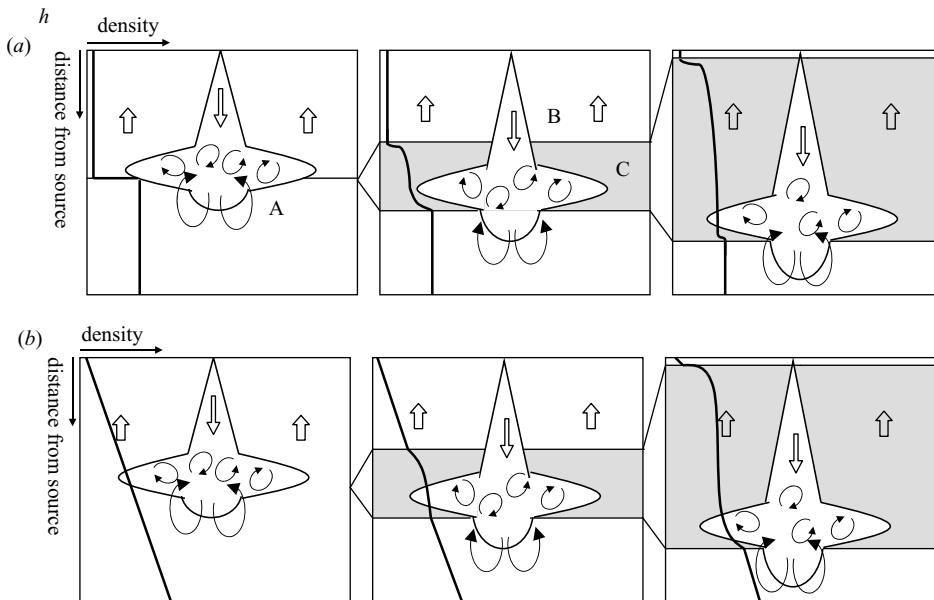
FIGURE 1. (*a*) In a two-layer stratification the plume initially spreads out along the interface forming an intermediate layer that gradually deepens through entrainment into the upper layer and through penetrative entrainment into the lower layer. (*b*) In a continuously stratified ambient, the plume is arrested and spreads out at the initial neutral height. The fluid above this layer, adjacent to the source, is then mixed through entrainment by the plume, while it gradually encroaches on the stratified fluid above as the plume becomes progressively more buoyant at the interface.

laboratory experiments in which we examine the mixing across a two-layer density interface produced by a strong intruding plume. We use a conductivity probe to describe in detail the time evolution of the density of the ambient fluid and we record the time at which the plume is able to break through the interface and descend through the lower layer. In §4, we develop a new phenomenological model to describe the evolution of the density profile in the ambient using a model advection–diffusion equation. This is based on the filling box advective flow coupled with the turbulent mixing of the ambient fluid surrounding the plume between the neutral buoyancy height and the maximum height of the plume. The mixing is assumed to be driven by the intruding flow produced by the plume, and to depend on the velocity and radial scale of the plume at the neutral height. We compare the predictions of the model with our new laboratory experiments. For comparison, we also adapt the model proposed by Kumagai (1984) for the penetrative entrainment across the interface coupled with the filling box advective flow, and we compare the results with our new advection–diffusion model.

In §5, we then apply our advection–diffusion model to examine the case of a plume mixing a continuously stratified ambient fluid. In the case of a continuously stratified environment, the mixing process is somewhat different, in that the plume initially advances to its neutral buoyancy height (Morton *et al.* 1956; Cardoso & Woods 1993). There is then an initial transient mixing period when the fluid between the source and the neutral buoyancy height becomes mixed (figure 1*b*). The time scale for this phase is given by the filling box time based on the distance between the source and the neutral buoyancy height (Baines & Turner 1969). Subsequently,

this mixed zone begins to deepen as the plume penetrates into the stratified zone and mixes the relatively dense fluid into this mixed layer. Cardoso & Woods (1993) developed a model for the long-time mixing of a stratified layer of fluid. However, their model did not account for the initial phase of the mixing, prior to the point at which the near-source layer had become approximately well mixed. In §5, we compare our new model predictions for the case in which a turbulent buoyant plume mixes a continuously stratified fluid, again using some new experimental data on the evolution of the density profile, collected using the conductivity probe. We then discuss some implications of the model for plume-driven mixing of a two-layer stratification within an enclosed room.

2. Scalings for a two-layer stratification

The classical theory of turbulent buoyant plumes (Morton *et al.* 1956) relates the source buoyancy flux B to the volume flux Q a distance H from the buoyancy source according to the relation

$$Q = \gamma B^{1/3} H^{5/3}, \tag{2.1}$$

where we work with top-hat profiles for the plume properties (cf. Morton *et al.* 1956), and $\gamma \sim 0.15$, is related to the entrainment coefficient α according to the relation $\gamma = (6\alpha/5)(9\pi 2\alpha/10)^{1/3}$, where α is the entrainment coefficient Morton *et al.* (1956).

Using this result, it follows that the buoyancy of the plume at the interface, $z = H_u$, has the form

$$g' = \gamma^{-1} B^{2/3} H_u^{-5/3}. \tag{2.2}$$

The buoyancy of the lower layer relative to the upper layer is given by

$$g'_l = g(\rho_l - \rho_u)/\rho_u.$$

Thus, the ratio of the initial buoyancy of the plume fluid at the interface to that of the lower layer is given by

$$\lambda = \left(\frac{B}{\gamma^{3/2} g^{3/2} H_u^{5/2}}\right)^{2/3} \frac{\rho_u}{(\rho_l - \rho_u)}. \tag{2.3}$$

In the context of the top-hat model, the mean motion of the plume is arrested at the interface if $0 < \lambda < 1$; otherwise it continues deep into the lower layer. In this paper, we focus on the case $0 < \lambda < 1$ when the plume is arrested at the interface, and our purpose is to describe the evolution of the deepening mixed layer. We re-interpret the ratio λ in terms of the two characteristic time scales of the flow. First, the filling box time τ_{fb} represents the time required for the plume to mix the upper layer, of depth H_u, adjacent to the plume source. This is given by the volume of the upper layer, divided by the volume flux of the plume at the interface

$$\tau_{fb} = \frac{A}{\gamma B^{1/3} H_u^{2/3}}. \tag{2.4}$$

Second, we can define the buoyancy time τ_b to represent the time required for the plume to increase the density of the upper layer to that of the lower layer in the case that the upper layer remains well mixed

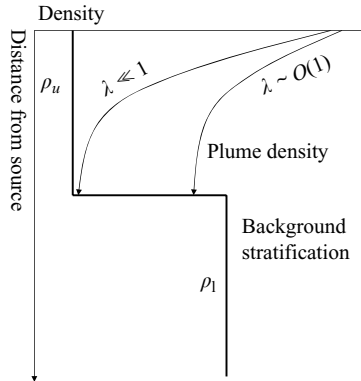$$\tau_b = \frac{AHg(\rho_l - \rho_u)}{B\rho_u}. \tag{2.5}$$

FIGURE 2. Illustration of the evolution of the density of the plume with depth, in the two different cases $\lambda \ll 1$ and $\lambda \sim O(1)$.

By inspection, we observe that

$$\lambda = \tau_{fb}/\tau_b. \tag{2.6}$$

In the limit $\lambda \ll 1$, which was studied in detail by Kumagai (1984), the plume is relatively weak. As it descends through the upper layer, it becomes even more dilute through entrainment. Therefore, at the interface, the buoyancy of the plume is much smaller than that of the lower layer. In this case, Kumagai (1984) showed that, long before plume breakthrough, the upper layer becomes approximately well mixed through the filling box process. As a result, the plume breakthrough time is approximately given by the time required for the density of the upper layer to evolve towards the density of the lower layer, namely, τ_b.

In his experimental description, Kumagai identified that prior to breakthrough, the plume in fact overshoots the interface between the layers and entrains a small amount of the lower layer fluid, which is then mixed into the upper layer. Kumagai modelled this process using an empirical entrainment law to describe the rate of entrainment of lower layer fluid by the plume into the upper layer; in his model, he assumed that the interface between the two layers remained sharp.

In the different limit $\lambda \sim O(1)$ with $\lambda < 1$, the plume is considerably stronger, and the buoyancy of the plume fluid at the interface may be close to that of the lower layer (figure 2). Initially, the plume fluid intrudes at the interface to form an intermediate layer which deepens upwards into the original upper layer. The density of the continuing plume at the interface with the lower layer progressively increases since the plume entrains progressively more fluid from this new intermediate layer, rather than the original upper layer. Eventually, on a time shorter than or comparable to the filling box time, the density of the plume at the interface with the lower layer becomes greater than that of the lower layer, and the plume then penetrates deep into the lower layer. An intermediate mixed zone is then left between the two original layers of fluid (figure 1). We now investigate the mixing in the case $\lambda \sim O(1)$ in more detail.

3. Experimental study of mixing a two-layer stratification

A series of experiments were carried out to explore the mixing of a two-layer stratification by a turbulent buoyant plume. Two tanks of different horizontal cross-section were used. Both tanks were 50 cm deep with tank A having a cross-section

$40\,\text{cm} \times 40\,\text{cm}$ and tank B a cross-section of $45\,\text{cm} \times 45\,\text{cm}$. For each experiment, the tank was initially filled with a 20–30 cm layer of aqueous salt solution, with concentration of order 1–3 wt%. A layer of fresh water, 15–25 cm deep, was then added to form a two-layer stratification. High salinity, aqueous solution was then supplied to the top surface of the fluid through a nozzle of diameter 5 mm; this was designed to produce a turbulent plume with a relatively small source volume flux compared to the volume flux entrained by the plume above the interface (cf. Woods, Caulfield & Phillips 2003). Fluid was supplied to the nozzle at a controlled rate using a peristaltic pump. A series of experiments were then conducted with a range of values for the plume buoyancy flux, designed so that at the interface, the density of the plume was intermediate between the upper and lower layer, taking a range of values of λ (§ 2).

In each experiment, the evolution of the vertical density profile was measured using a conductivity probe. This carried out a vertical traverse of the tank every 1–2 min. The probe requires 10–15 s per traverse while the typical filling box time was 300–1000 s, so that each profile gives a representative snapshot of the density profile when viewed over the time scale of the mixing. In measuring the conductivity, fluid is siphoned through the probe, and the changing salinity of the fluid entering the probe leads to a changing voltage signal from the instrument. This is calibrated with a series of standard aqueous solutions of known salinity, in order to convert the voltage signal to salinity. In each experiment, the time of breakthrough τ_b was defined as the time at which the plume fluid first spread out at the base of the tank. Immediately prior to this transition, some of the fluid did penetrate through the interface and mix, but then rose back up towards the interface, in a somewhat analogous fashion to that reported by Kumagai (1984).

Prior to the main experiments, we carried out a series of calibration experiments for the plume source used herein, to measure the value of α for the turbulent buoyant plume (1.1). In these experiments, the plume descended through a single layer of fluid 40 cm deep, and we recorded the rate of ascent of the so-called first front, associated with the deepening layer of fluid which is supplied to the base of the tank by the plume (Baines & Turner 1969). The position of this front is described analytically as

$$t = \frac{3A}{2B^{1/3}\gamma z_0^{2/3}}\left(1 - \left(\frac{z_0}{z}\right)^{2/3}\right), \tag{3.1}$$

where A is the cross-sectional area of the tank, and the position z includes a virtual origin correction z_0 which is calculated following the approach of Hunt & Kaye (2001). By comparing the experimental data with the model, we estimate that $\gamma = 0.15$ which is consistent with published data (Morton *et al.* 1956, Baines & Turner 1969). It was found that the source parameter $\Gamma = (5Q_0 2B_0)/(8\sqrt{2\pi}\alpha M_0^{5/2})$ had a value of order 1 or greater, indicating that in the present experiments the plume was close to pure-plume balance (cf. Caulfield & Woods 1995; Hunt & Kaye 2001). In the experiments, the virtual origin of the source was found to have value of order $z_v \sim 1.0\,\text{cm}$.

The detailed experimental parameters for each experiment are listed in table 1. This table also shows the value of λ for each experiment. The experiments we carried out spanned the range of λ from 0.04 to 0.65. In figure 3 we illustrate how the salinity profile evolves with time once the plume flow commences, for the cases $\lambda = 0.1$ and 0.3. The salinity has been scaled relative to the initial salinity contrast between the upper and lower layer, and the depth relative to the distance between the plume source corrected for a virtual origin and the initial interface position. Also, in the figure, the

Experiment number	Tank	B_0 (10^{-6} m^4 s^{-3})	Q_0 (10^{-6} m^3 s^{-1})	H (m)	Δ_2 (m s^{-2})	λ	t_b (s)	Γ
1	A	2.94	2.00	0.170	0.087	0.32	380	1.30
2	A	2.94	2.00	0.166	0.105	0.27	510	1.30
3	A	2.85	1.93	0.164	0.141	0.20	740	1.41
4	A	1.42	0.96	0.124	0.141	0.20	N/A	5.69
5	A	1.42	0.96	0.147	0.070	0.30	N/A	5.69
6	A	2.82	1.91	0.152	0.105	0.30	N/A	1.43
7	A	2.84	1.93	0.163	0.070	0.40	285	1.40
8	A	1.62	1.10	0.114	0.087	0.40	N/A	4.32
9	A	1.59	1.08	0.195	0.141	0.10	1924	4.48
10	A	0.44	0.61	0.157	0.087	0.10	N/A	6.88
11	A	2.93	1.99	0.124	0.070	0.64	116	1.31
12	A	2.93	1.99	0.142	0.070	0.51	180	1.31
13	A	1.41	1.97	0.146	0.141	0.15	1498	0.65
14	B	1.41	1.99	0.164	0.141	0.20	740*	0.64
15	B	2.93	1.96	0.142	0.070	0.51	180*	1.38
16	B	1.41	1.97	0.146	0.141	0.15	1498*	0.65

TABLE 1. Experimental runs. The values for H include a virtual origin correction.

profiles have been offset along the x-axis by a distance proportional to the time at which that profile was recorded in order to aid visualization of the evolution of the profiles. In both cases, results are shown from two experiments in which the source fluid has different initial buoyancy flux, upper layer depth and density difference between layers, but the same value of λ. The close overlap of the two sets of data for a fixed value of λ illustrates that this is a key controlling parameter.

The figure shows that once the plume intrudes at the interface, a zone of intermediate density gradually develops and deepens, both upwards and downwards. Visual observations show that the plume overshoots the interface, mixes with some of the lower layer fluid and then rises back to the interface zone where it intrudes laterally to form an intermediate layer of mixed fluid (figure 4). The rate of deepening of this layer back towards the plume source is faster than the rate of deepening into the lower layer of fluid. However, the mixed zone does progressively advance into the lower layer. As expected, eventually the plume penetrates through the interface and then continues to descend through the lower layer.

The time at which the plume penetrates the interface and descends through the lower layer depends on the value of λ. In figure 5, we present a summary of our experimental observations of the plume breakthrough time τ_p as a function of λ. The breakthrough times are scaled relative to the buoyancy evolution time for the upper layer τ_b (§1). In this figure we also include the data presented by Kumagai (1984) from his experiments, which were limited to the range $0 < \lambda < 0.15$. It is seen that in the limit of small λ, the breakthrough time is essentially independent of λ, and has value $\tau_p \sim \tau_b$. In this limit, the plume is very weak, so the fluid at the interface has a value similar to that of the upper layer, and therefore in order to breakthrough, the buoyancy of the whole upper layer needs to evolve to that of the lower layer. For large values of λ however, the plume density is much closer to that of the lower layer. As a result, plume breakthrough occurs once a relatively thin intermediate layer has formed, and so the time for breakthrough becomes much shorter than the time required for the buoyancy of the whole upper layer to evolve to that of the lower layer τ_b. The solid and dashed lines correspond to the prediction of our new

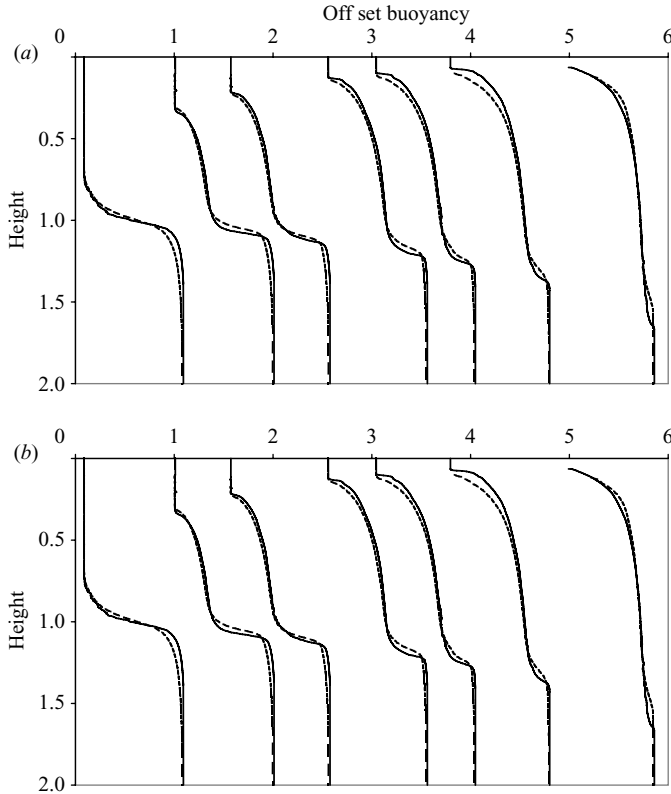FIGURE 3. Profiles of the density variation with depth in the ambient fluid. The curves have been offset according to the time of the measurement τ to indicate the time evolution of the system, so that, in the data, the x coordinate has the form $x = (\rho_a(z) - \rho_t)/(\rho_b - \rho_t) + \delta\tau$. The height has been scaled with the initial distance of the interface from the source. For each graph two experiments were run with the same value of λ, and the two sets of data have been plotted to illustrate that the dynamics depend only on λ and to show repeatability and level of error. (*a*) In this figure, $\lambda = 0.1$ and the data for experiment 9 are shown with solid lines, and experiment 10 is shown with dashed lines. Profiles are shown at dimensionless times $\tau = 0$, 1.24, 1.93, 3.15, 3.75, 4.68, 5.98, $\delta = 0.81$. (*b*) In this figure, $\lambda = 0.3$ and the data for experiment 5 are shown with solid lines, and experiment 6 is shown with dashed lines. Profiles are shown at dimensionless times $\tau = 0.03$, 0.29, 0.81, 1.11, 1.48, $\delta = 4.3$.

advection–diffusion model and our adaptation of the Kumagai (1984) model, which we describe in the next section. We note here, however, that both models are based on the mixing and entrainment in a turbulent buoyant plume, and it is this plume which dominates the supply of fluid to the deepening intermediate layer; even though the two models describe the details of the penetrative mixing with the lower layer in a different way, the evolution of the density of the plume at the interface with the lower layer is controlled by the plume entrainment as it descends from the source. As a result, both models provide a reasonable estimate of the data on the time for breakthrough.

For convenience of empirical modelling in applications of this work, we have also developed a simple curve fit through the data

$$\tau_p = \tau_b(0.4\mathrm{e}^{-7\lambda} + 0.6(1 - \lambda)) \tag{3.2}$$

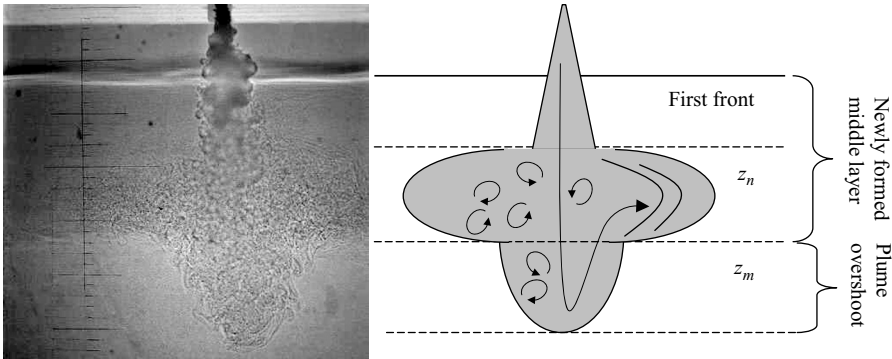which is accurate within 1 % of each of the experimental data.

FIGURE 4. A typical photograph of the most distant part of the plume from the source, taken during experiment 2. The figure illustrates the turbulent mixing of fluid in the region of plume arrest as illustrated on the adjacent schematic of the mixing.
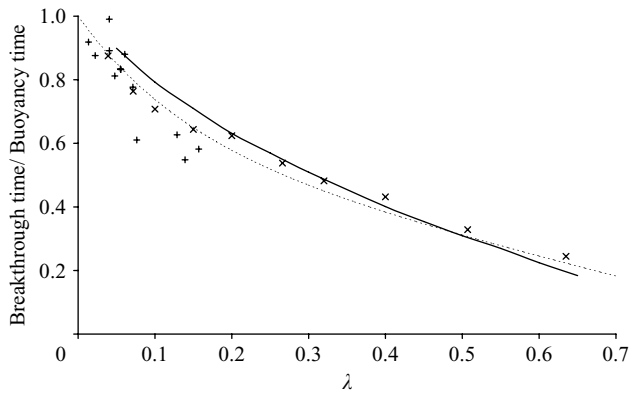

FIGURE 5. Dimensionless plume breakthrough time as a function of λ. Time has been scaled with the buoyancy time τ_b (2.5). The symbols $\times$ show experimental data points. The symbols $+$ show data points from Kumagai (1984). The solid line represents the prediction of the new advection–diffusion model described in §4, the dashed line represents the prediction from the adaptation of the Kumagai (1984) model.

4. The model for mixing

We now develop a phenomenological model for the formation of the intermediate mixed layer based on the combined action of the filling box return flow and the mixing associated with the intrusion of plume fluid in the interface region. To place our model in context, it is useful to review some of the previous literature.

The original modelling approach of Baines & Turner (1969), which has been adopted by many subsequent workers (Kumagai 1984; Cardoso & Woods 1993) assumes that the intrusion occurs at a specific depth, with a sharp interface, and that iso-density surfaces are then advected by the filling box return flow back towards the source. In order to capture the effects of penetrative entrainment, these models then introduce a law for the entrainment of fluid from below the interface. This entrained fluid is assumed to mix with the plume fluid just prior to forming the new intruded layer. As the plume continues, the density of the plume arriving at the interface gradually evolves, and as a result, the intermediate layer becomes stratified, with a sharp density interface at both the upper and lower surfaces of the intermediate layer

Kumagai (1984). We have used the model for penetrative entrainment proposed by Kumagai (1984) to calculate the entrainment by the plume across the interface between the intermediate layer and the original lower layer. We have then combined this with the model of a turbulent buoyant plume moving through a stratified environment in order to predict the plume volume flux as a function of position and time. This leads to a model for the evolution of the ambient density profile $\rho_a(z, t)$ in the region above the interface with the lower layer fluid $z < h_i$, say, given by

$$\frac{\partial \rho_a}{\partial t} + w \frac{\partial \rho_a}{\partial z} = 0, \tag{4.1}$$

where the advection in the ambient fluid is driven by the plume volume flux, $w(z) = -Q(z)/A$, with $Q(z)$ the plume volume flux and A the area of the container. The plume volume flux is calculated using the model for a turbulent buoyant plume (Morton *et al.* 1956; Turner 1979) in which the volume flux $Q(z)$, the momentum flux $M(z)$ and the buoyancy flux $B(z)$ evolve as the plume descends from the source, through the ambient flux, with local stratification $N2 = -(g/\rho)(\mathrm{d}\rho_a/\mathrm{d}z)$, according to the conservation laws

$$\frac{\mathrm{d}Q}{\mathrm{d}z} = 2\alpha M^{1/2}; \quad M \frac{\mathrm{d}M}{\mathrm{d}z} = FQ \quad \text{and} \quad \frac{\mathrm{d}B}{\mathrm{d}z} = -N2Q. \tag{4.2}$$

Following Kumagai (1984), the rate of entrainment of lower layer fluid $Q_e = Fr3/(1 + 3.1Fr2 + 1.8Fr3)$ across the lower layer $z = h_i$ is given in terms of the Froude number $Fr = M^{5/4}/Q^{3/2}\Delta^{1/2}$ evaluated at the interface where Δ is the buoyancy jump across the interface. As a result, the interface with the lower layer, $z = h_i$, then descends at a rate given by

$$A \frac{\mathrm{d}h_i}{\mathrm{d}t} = Q_e. \tag{4.3}$$

In figure 6, the predictions for the evolution of the density profile from this model are shown in comparison to the experimental data for $\lambda = 0.1, 0.3$ and 0.4, at a series of times during the experiment. The experimental data suggests that the density profile evolves in a more spatially continuous fashion rather than there being a jump in density at the interface with the lower layer.

Indeed, observations of the experiments (figure 4), and the density profiles presented in figure 3, suggest that the penetration of the plume across the interface and the subsequent fall back towards the neutral buoyancy height is intermittent and spatially distributed. The plume fluid appears to intrude at the neutral height, but the turbulence in the fountaining flow also appears to create a mixing zone just outside the ascending plume, between the neutral height and the top height of the plume, over a lateral dimension which scales as the plume radius (figure 4).

Measurements of turbulent buoyant plumes suggest that the turbulent velocity fluctuations in the plume scale with the characteristic velocity of the plume (Papanicolaus & List 1988); this scaling is also likely to control the turbulent velocity fluctuations in the fountaining flow around the plume top. We therefore expect that as a result of the fountaining, in the region between the plume top and the neutral height, there is a vertical buoyancy flux associated with the mixing F_b, which scales as

$$F_b = \epsilon u b \frac{g}{\rho_0} \frac{\partial \rho}{\partial z} b^2, \tag{4.4}$$

where ϵ is a dimensionless parameter, u is the mean velocity and b the radius of the plume. Owing to the stratification, we expect that any mixing beyond the plume
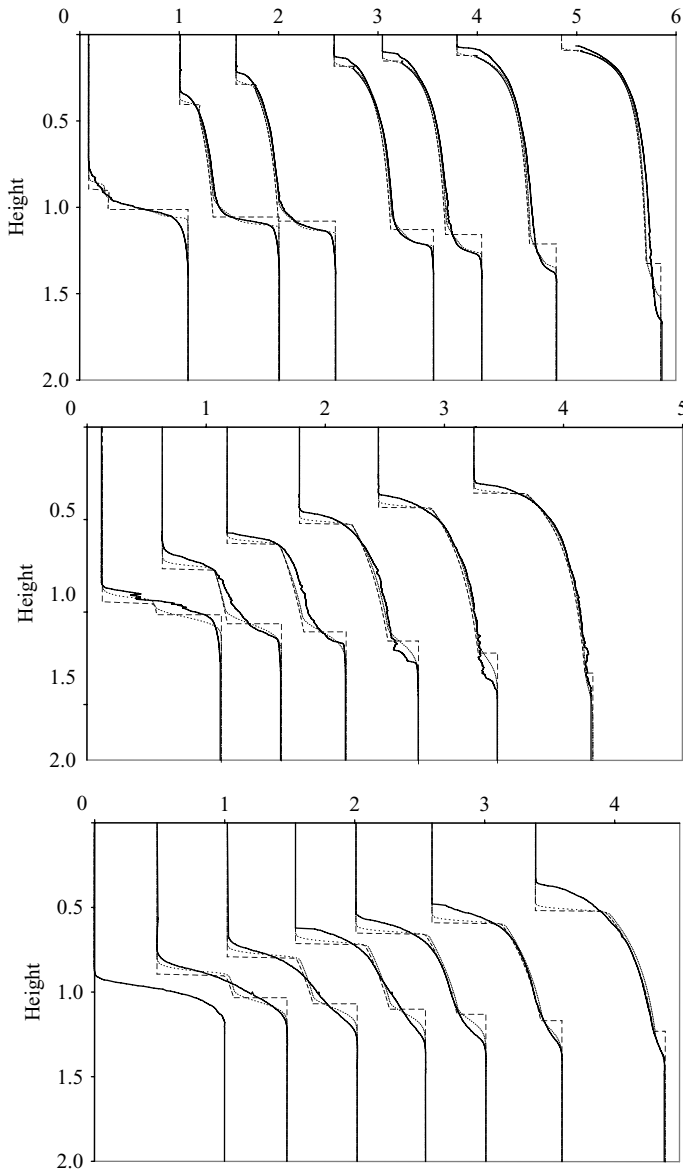
FIGURE 6. Evolution of the density profiles in the ambient fluid for three experiments in which $\lambda = 0.1, 0.3$ and 0.4. In each experiment, the measured profiles (solid lines) have been offset along the x-axis a distance proportional to the time after the start of the experiment when that profile was measured, so that the x-coordinate has the form $x = (\rho(z) - \rho_t)/(\rho_b - \rho_t) + \delta\tau$. The height has been scaled with the initial distance of the interface from the source. The predictions of both the Kumagai model (dashed) and new model for mixing (dotted) are also shown here at each of the times that the density profiles were measured. (*a*) Shows $\lambda = 0.1$. At times $\tau = 0, 1.24, 1.93, 3.15, 3.75, 4.68, 5.98$ with $\delta = 0.81$. (*b*) Shows $\lambda = 0.3$. At times $\tau = 0.03, 0.29, 0.81, 1.11, 1.48$ with $\delta = 4.3$. (*c*) Shows $\lambda = 0.4$. At times $\tau = 0.12, 0.25, 0.37, 0.49, 0.63, 0.82$ with $\delta = 4.1$.

top or nearer the plume source than the neutral buoyancy height will decay. The characteristic distance over which such mixing would decay, l say, may depend on a balance between the kinetic energy available for mixing and the potential energy

required for mixing, leading to a relation of the form

$$l = \frac{\beta u}{((g/\rho_o)(\partial\rho/\partial z))^{1/2}}, \tag{4.5}$$

where β is a constant of proportionality. Since the stratification varies with height, we expect the extent of the decaying zone to be different adjacent to the neutral buoyancy height and adjacent to the maximum height of the plume, and so we calculate l using the local gradient $(\partial\rho/\partial z)$ at each of these levels, giving the decay scales l_n and l_m near the neutral and maximum heights of the plume.

Using this phenomenological model for the mixing, we can express the coefficient ϵ, given in (4.1) for the flux, in the form

$$\epsilon = \begin{cases} \epsilon_0 \exp(-(z-z_n)^2/l_n^2) & z < z_n \\ \epsilon_0 & z_n < z < z_m \\ \epsilon_0 \exp(-(z-z_m)^2/l_m^2) & z_m < z \end{cases} \tag{4.6}$$

where z_n and z_m are the neutral and maximum heights of the plume. This model has two dimensionless constants ϵ_o and β, which represent the ratio of the turbulent velocity fluctuations relative to the mean, and the constant of proportionality in the length scale over which the turbulent mixing decays (4.5).

We now combine this model for the vertical mixing of buoyancy with the advection of the ambient fluid associated with the filling box flow to infer that over the whole cross-section of the tank A, the density evolves according to the conservation law

$$\frac{\partial\rho}{\partial t} + w(z)\frac{\partial\rho}{\partial z} = \frac{\partial}{\partial z}\left(\epsilon \frac{ub^3}{A}\frac{\partial\rho}{\partial z}\right). \tag{4.7}$$

In order to calculate the characteristic speed and radius of the plume, we again draw from the classical theory of turbulent buoyant plumes rising through a stratified environment (Morton *et al.* 1956) (4.2). We also note that the product of the mean speed and radius is related to the momentum flux according to the relation $ub = M^{1/2}$.

In the model, during each time step, we update the ambient density field and we then solve the plume equations to find the neutral height of the plume z_n, at which $B = 0$, and the top height of the plume z_m, at which $M = 0$. We then use the values of Q and M at the neutral buoyancy height to determine the turbulent velocity and hence the effective turbulent mixing coefficient (4.6). This value is used together with the updated plume volume flux as a function of height as inputs for the advection–diffusion equation (4.7). In solving this equation, we also assume that the fluid supplied by the plume intrudes to form a discrete layer at the neutral height z_n. The turbulent mixing described above then redistributes this fluid across the mixing zone.

The model for the diffusive mixing has two empirical constants ϵ_0 and β. Comparison with a series of data sets for the cases $\lambda = 0.1, 0.2, 0.3$ and 0.4 suggests that the optimal fit to the data is achieved by setting $\epsilon_0 = 0.32$ and $\beta = 2.2$.

We compare the predictions of this advection–diffusion model (dotted) with the experimental density profiles (solid) in figure 6(*a–c*). Given the variability between experiments (e.g. figure 3) the agreement between theory and experiment is good, especially at the interface with the original lower fluid layer, where the model predicts formation of a continuous density profile as the plume entrains the lower layer fluid into the new intermediate layer. In contrast, the penetrative entrainment model adapted from the work of Kumagai (dashed line) predicts that a sharp interface develops at the interface with the lower layer. One area of discrepancy between our model (dotted line) and the new data is that in the experiments there is a somewhat

smoother adjustment of the density profile between the upper (near source) layer and the new intermediate layer. Although part of this may be associated with experimental variability, there may be some additional mixing of near source fluid as the fountaining flow overshoots the neutral height, and this mixing may be enhanced by the density fluctuations within the fountaining flow (Baines, Corriveau & Reedman 1993; Ansong, Kyba & Sutherland 2008). However, given the reasonably successful agreement of the present phenomenological mixing model, both for the density profiles and the plume breakthrough time, based on the simplified top-hat model for a plume, we have resisted incorporating any further parameterisations to describe this.

As well as the detailed density profiles, the models are reasonably successful in predicting the time at which the plume breaks through the interface and penetrates into the lower layer. The new advection–diffusion model (dotted line) is perhaps a little more accurate than the adapted Kumagai model (dashed line) in predicting the breakthrough point as measured in our experiments, especially in the case of larger λ, as shown by the solid line in figure 5. However, both models are in reasonable accord with the experimental data.

5. Continuous stratification

Up to this point, we have focused on the mixing across a two-layer density interface. However, in general, the ambient density may vary continuously with height. It is therefore of interest to test the applicability of the advection–diffusion model in the complementary problem in which the ambient fluid is initially continuously strati-fied. This problem has previously been studied by Cardoso & Woods (1993) who combined the theory of turbulent buoyant plumes with a model for penetrative entrainment at the top of the plume based on the conversion of kinetic energy of the plume fluid to potential energy. Their model applies in the long-time limit such that the filling box process has mixed the ambient fluid in the region below the top of the plume; indeed in their model, it is assumed that this region is well mixed. However, in the early stages of the mixing, the plume rises through the stratified ambient to its initial neutral height. The initial intrusion height is given in terms of the buoyancy flux B and ambient stratification N by (Morton *et al.* 1956)

$$H \sim 2.5 B^{1/4} N^{-3/4}. \tag{5.1}$$

As the plume continues, the intruding layer gradually deepens and, over a filling box time, it mixes the ambient fluid between the source and the neutral height. The filling box time associated with the plume volume flux at height H may be written (§2) as

$$\tau_f \simeq \frac{A}{\gamma B^{1/3} H^{2/3}}. \tag{5.2}$$

Once this layer has become well mixed, the mixing process is well described by the simplified model proposed by Cardoso & Woods (1993), but that model does not describe the evolution of the stratification in the early stages of the mixing while the near-source region is stratified. However, our new advection–diffusion model, introduced in §4, can be applied to this different flow regime and we now compare the predictions of the model with some new experimental data for the evolution of the density profile as a stratified region is mixed by a turbulent plume.

To this end, we have conducted a series of new experiments in which a continuously stratified ambient was mixed by a turbulent buoyant plume, and the evolution of the

Experiment number	Tank	B_0 (10^{-6} m^4 s^{-3})	Q_0 (10^{-6} m^3 s^{-1})	N (s^{-1})	Γ
17	B	1.93	1.31	0.54	3.04
18	B	1.42	0.97	0.46	5.52
19	B	2.93	2.00	0.48	1.30

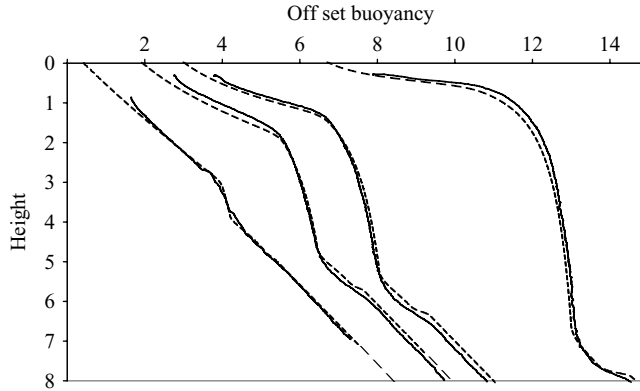TABLE 2. Experimental runs of a continuous stratification.

FIGURE 7. Evolution of the vertical density profiles in the tank, as measured during experiment 15. Each profile has been offset according to the time of measurement compared to the prediction of the new advection–diffusion model for the mixing $(\rho(z) - \rho_t)/(\rho_b - \rho_t) + \delta\tau$. Height has been scaled with $H = 2^{-7/8}\pi^{-1/4}\alpha^{-1/2}B^{-1/4}N^{-3/4}$ (Cardoso & Woods 1993). For experiment 15 with a continuous stratification. At times $\tau = 0.15$, 0.75, 1.14, 2.53, $\delta = 2.64$.

density profile was recorded using the conductivity probe. In figure 7, we compare the density profiles at four times, $\tau = 0.15$, 0.75, 1.14 and 2.53 for a typical experiment 18, as listed in table 2. We have also plotted the prediction of the new mixing model for this experiment, as shown by the solid lines. The parameters ϵ_o and β correspond to those given in §4 for the mixing of a two-layer interface. It is seen that there is good agreement between the model predictions and the experimental data at both short and long times. As well as describing the short-term mixing of the region below the initial neutral buoyancy height of the plume, the model provides a very accurate description of the mixing across the density jump between the mixed layer and the overlying continuously stratified ambient fluid.

6. Application

One important application of this modelling relates to quantification of the transient mixing within buildings produced by turbulent buoyant plumes. Often in buildings there may be a density gradient through the space, perhaps owing to a vertically distributed heat load, or owing to buoyancy-driven displacement ventilation from localized heat sources (Cooper & Linden, 1996; Linden 1999). It is interesting to calculate the values of λ associated with heat sources of different strength rising through such an ambient stratification, to determine whether a plume will break through the stratification, or will fully mix the near-source zone until the temperature contrast between the layers is much smaller. This has an impact on the thermal comfort of the occupants, typically located in the lower part of the space. We
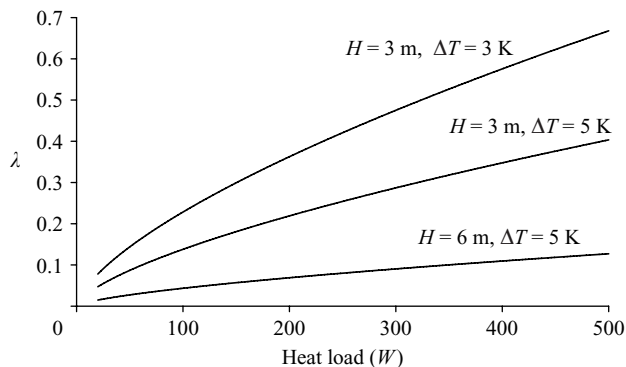
FIGURE 8. The value of λ for a range of heat loads in a room containing a two-layer stratification with interface height H and temperature difference ΔT.

consider the idealized case of a warm plume rising into a two-layer stratification, noting that in buildings with multiple quasi-steady heat sources there may be many discrete layers (cf. Cooper & Linden 1996; Linden & Cooper 1996).

In figure 8 we show the value of λ as a function of the heat load, for a localized source with strength in the range 0–500 W, rising through an environment with a two-layer stratification with an interface at height 3 or 6 m above the source, and with a temperature contrast of 1 or 3 K. It is seen that with the larger heat loads, perhaps associated with larger office equipment (large printers, photocopiers etc.) λ lies in the range 0.2–0.5, and so the plume will partially mix the interface zone, but then penetrates to higher level. In contrast, the smaller heat loads, such a desktop pc's which produce 100–200 W have values of λ in the range 0.001–0.1, and so are unlikely to penetrate the stratification. Instead they heat up the lower layer of air until the temperature becomes much closer to the upper layer and the stratification becomes eroded. This difference in behaviour of the small and large heat loads can be very important in determining how stratified the interior ambient fluid may become.

7. Conclusions

We have explored the mixing of a stratified confined layer of fluid by a turbulent buoyant plume with some new experiments which identify how the detailed density profile evolves with time. A key observation is that with a strong plume, such that the density of the plume relative to the upper layer is comparable to the density of the lower layer, there is a short period during which an intermediate layer of mixed fluid deepens between the upper and lower layers, but subsequently the plume penetrates through the interface and descends into the lower layer. In contrast, with a weak plume, the plume is arrested at the interface and a filling box type flow mixes the plume fluid through the upper layer, until the upper layer bulk density has increased to a value comparable to the lower layer. Then the plume penetrates through the interface into the lower layer.

Motivated by this new data, we have developed a model for the mixing of a stratified region of fluid by a localized turbulent buoyant plume, based on the combined action of the filling box flow and the effective turbulent diffusivity associated with the conversion of the kinetic energy of the plume fluid to potential energy in the plume. The new model predictions are in good accord with our new experimental data for

the mixing of a two-layer stratification and also for the mixing of a continuously stratified region.

For comparison, we have also adapted the earlier model for mixing of a two-layer stratified ambient by a weak plume, as proposed by Kumagai (1984), for the case in which there is a relatively strong plume; this also provides a reasonable model of the mixing process except for the prediction of a sharp density jump with the original lower layer. In contrast, our new model, which includes a diffusive mixing term associated with the turbulence in the fountain, is able to predict the development of the continuously stratified zone near the original lower layer of fluid.

Also, for the case of a continuously stratified ambient, we have compared the new model with an earlier model proposed by Cardoso & Woods (1993), in which the region between the source and the height at which the plume intrudes laterally was modelled as being well mixed. The main advance of the new model is that it can describe the initial transient mixing of the ambient fluid in the region between the source and the height at which the plume fluid intrudes laterally; both models do however provide an accurate prediction of the subsequent long-time mixing when the region between the source and the height at which the plume intrudes laterally into the ambient fluid is indeed well mixed.

There are many problems for which the modelling of this transient mixing may be important. For example, in the context of building ventilation, a weak, but hot plume may be trapped in the lower part of a thermally stratified room, and if this lower region continues to warm up, it could compromise the thermal comfort of the occupants. Also, there are applications in which chemical reactions may result from plume-mixing processes within confined spaces (Conroy *et al.* 2005); as understanding of the transient mixing processes improves, the ability to control such reactions, or limit exposure to the results of such reactions may also improve. Finally, we note that there are a number of geophysical contexts in which mixing produced by plumes at density interfaces is important, and we are presently developing models of such processes.

REFERENCES

Ansong, J. K., Kyba, P. J. & Sutherland, B. R. 2008 Turblent fountains in a closed chamber. *J. Fluid Mech.* **595**, 115–139.

Baines, W. D., Corriveau, A. F. & Reedman, T. J. 1993 Turblent fountains in a closed chamber. *J. Fluid Mech.* **255**, 621–646.

Baines, W. D. & Turner, J. S. 1969 Turblent buoyant convection from a source in a confined region. *J. Fluid Mech.* **37**, 51–80.

Cardoso, S. S. S. & Woods, A. W. 1993 Mixing by a plume in a confined stratified region. *J. Fluid Mech.* **250**, 277–305.

Caulfield, C. P. & Woods, A. W. 1995, Plumes with non-monotonic mixing behaviour. *Geophys. Astrophys. Fluid Dyn.* **79**(1–4), 173–199.

Conroy, D. T., Llewellyn Smith, S. G. & Caulfield, C. P. 2005, Evolution of a chemically reacting plume in a ventilated room. *J. Fluid Mech.* **537** 221–253.

Cooper, C. P., & Linden, P. F. 1996, Natural ventilation of an enclosure containing two buoyancy sources. *J. Fluid Mech.* **311**, 153–176.

Fitzgerald, S. D. & Woods, A. W. 2007 Transient natural ventilation of a room with a distributed heat source. *J. Fluid Mech.* **591**, 21–42.

Hunt, G. R. & Kaye, N. E. 2001 Virtual origin correction for lazy turbulent plumes. *J. Fluid Mech.* **435**, 377–396.

KUMAGAI, M. 1984 Turbulent convection in a two-layered region. *J. Fluid Mech.* **147**, 105–131.

LINDEN, P. F. 1999 The fluid mechanics of natural ventilation. *Annu. Rev. Fluid Mech.* **31**, 201–238.

LINDEN, P. F & COOPER, P. 1996, Multiple sources of buoyancy in a naturally ventilated enclosure. *J. Fluid Mech.* **311**, 177–192

MORTON, B. R., TAYLOR, G. I. & TURNER, J. S. 1956 Turbulent gravitational convectoin from maintained and instantaneous sources. *Proc. R. Soc. Lond.* A **234**, 1–23.

PALUSKIIEWICZ, T., GARWOOD, R. W. & DENBO, D. W. 1988 Deep convective plumes in the ocean. *Oceanography* **7**, 37–44.

PAPANICOLAOU, P. N. & LIST, E. J. 1994 Investigations of round vertical turbulent buoyant jets. *J. Fluid Mech.* **195**, 341–391.

PHILLIPS, J. C. & WOODS, A. W. 2001 Bubble plumes generated during recharge of a basaltic magma chamber. *Earth Planet Sci. Lett.* **186**, 297–309.

TURNER, J. S. 1979 *Buoyancy Effects in Fluids,* pp. 165–206. Cambridge University Press.

WOODS, A. W. & PHILLIPS, J. C. 1999 Turbulent bubble plumes and CO_2 driven lake eruptions. *J. Volcanol. Geothermal Res.* **92**, 259–270.

WOODS, A. W., CAULFIELD, C. P. & PHILLIPS, J. C. 2003 Blocked natural ventilation: the effect of a source mass flux. *J. Fluid Mech.* **495**, 119–133.